

# **A Simple Theory of Viscosity in Liquids**

Jean Bellissard\*

School of Mathematics and School of Physics, Georgia Institute of Technology, Atlanta GA,  
USA, and

Fachbereich Mathematik und Informatik, Westfälische Wilhelms-Universität, Münster, Germany

Takeshi Egami

Department of Materials Science and Engineering and Department of Physics and Astronomy,  
University of Tennessee, Knoxville, TN 37996, USA, and

Oak Ridge National Laboratory, Oak Ridge, TN 37831, USA

\*E-mail address: jeanbel@math.gatech.edu

## **Abstract**

A simplistic model of atomic dynamics in liquid, based on the concept of dynamic fluctuations in local atomic connectivity, is proposed to elucidate the temperature variation of the viscosity of a material in its liquid phase. Within the simplifications and hypothesis made to define the model, it is possible to explain the crossover from a simple liquid to a cooperative liquid and covariance of viscosity near the glass transition temperature. The model is a mechanical analog of the Drude model for the electric transport in metal.

## 1. Introduction

Viscosity,  $\eta$ , of a liquid near the melting point is of the order of  $10^{-3}$  Pa.s, whereas the glass transition is defined by  $\eta$  reaching  $10^{12}$  Pa.s [1]. The origin of this rapid change in viscosity over a relatively small range of temperature is crucially related to the unsolved problem regarding the nature of the glass transition [2, 3]. In spite of numerous attempts to explain its origin [4-9] there is no broad agreement on this subject. Whereas much attention is currently focused on the behavior of highly viscous supercooled liquids, in our view the most important feature of the viscosity is the crossover from the Arrhenius to super-Arrhenius behavior which occurs at a temperature,  $T^*$ , much higher than the glass transition temperature,  $T_g$ . Kivelson noted that the temperature dependence of the activation energy is universal if  $T^*$  is used to scale temperature [6]. The functional form of the universal behavior explains quite well the measured viscosity of a large number of metallic alloy liquids [10]. Once the temperature dependence of the viscosity becomes super-Arrhenius and the activation energy keeps increasing with decreasing temperature, and it is a natural course of action that viscosity diverges at a finite temperature. The glass transition is merely a consequence of this crossover. Therefore in this line of argument the crucial element for understanding the glass transition is not the glass transition itself but the nature and origin of this crossover phenomenon.

Kivelson proposed that  $T^*$  is the freezing temperature of a phase to which the liquid never reaches because of frustration [6]. Because of its intrinsic frustration long-range order of such a phase cannot be achieved, but short-range dynamic fluctuations into this phase become more prevalent as temperature is lowered, resulting in increased viscosity and ultimate jamming into a glassy state. An example of the frustrated phase is the icosahedral state [4, 11]. Whereas a quasicrystal is a solid with icosahedral symmetry, it is a stoichiometric crystalline compound in six dimensions which is formed only for a number of specific compositions [12]. For a liquid with a composition other than these specific compositions the icosahedral order is geometrically frustrated [4], and cannot form long-range order. But the particular local order of the frustrated phase depends on composition. For instance for a poly-dispersed hard-sphere colloids the fluctuating phase is a mixture of the icosahedral phase and the *f.c.c.* phase [13]. However, the hypothesis that  $T^*$  is the freezing temperature of the frustrated phase has not been confirmed.

On the other hand different interpretations of the crossover phenomenon were proposed based upon the idea that the atomic dynamics become more collective below  $T^*$  [14, 15]. Such

crossover is observed in colloidal system as well, as a function of colloid density, from non-interacting colloid below the critical density to interacting colloid above [16, 17]. In our view the crossover occurs when the mean-free path of shear phonon,  $\xi = c_T \tau_M$ , where  $c_T$  is the velocity of a transverse phonon and  $\tau_M$  is the Maxwell relaxation time, becomes shorter than the mean atomic distance, the bulk of shear phonons are localized [15]. In other words above the crossover temperature,  $T_A = T^*$ , the structure is fluctuating so fast that phonons cannot propagate and become overdamped. Only below  $T_A$  atoms can interact via phonons and atomic dynamics becomes cooperative. In this paper we propose a simple model to quantify this dynamic crossover phenomenon based on the dynamics of atomic connectivity network. We define the structure of liquid in terms of the atomic connectivity network [18], and describe its dynamics by the action of cutting and forming the atomic bond [19]. The crossover occurs as a consequence of competition between phonons and bond cutting. This model is a mechanical analog of the Drude model for the electric transport in metal. The work presented here is a small brick added to the knowledge, hoping that it will open the door to a more accurate theory liable to explain the mystery of glass transition. However, several evidences point toward this model providing some universal results: (a) it explains the crossover phenomenon, (b) it introduces a parameter that permits to distinguish between strong and fragile glasses, and (c) it explains the precipitous increase in viscosity below the crossover temperature. In addition, while being first motivated by the study of bulk metallic glasses, it could be relevant in other areas, such as colloids [20], usual glassy materials in their liquid phase, or even quantum fluids [21].

## 2. The model

### 2.1. Structure and dynamics of liquid

Liquid and glass has no symmetry in the atomic structure. Thus it is difficult to describe the structure and relate it to properties, even when we know the positions of all atoms at time  $t$ ,  $\mathbf{R}_i(t)$ . Experimentally the only the pair density correlation function (PDF),  $g(r)$ , can be readily obtained through the Fourier-transformation of the structure function,  $S(Q)$ , which can be determined by diffraction [22]. However, the PDF is a one-dimensional function, and does not have sufficient informational content to determine a three-dimensional structure. To describe the three-dimensional structure usually a model is constructed using a phenomenological interatomic potential, and the results are analyzed in terms of the Voronoi polyhedra [18, 23], which is an

example of the Delone set [24, 25], as discussed in Appendix 1. The atomic connectivity is defined by atoms which share a Voronoi face. The state of atomic connectivity is expressed in terms of the Delone graph.

Now the Delone graph describes the state of atomic connectivity at a time. We now consider how it evolves with time to describe its dynamics. The action of changing the connectivity of the Delone graph, by cutting one bond and forming a new one, is called Pachner moves discussed in Appendix 2 [24 – 27]. Such a move requires local atomic rearrangement which squeezes atoms and increases the potential energy. It represents a move from one local equilibrium to another, crossing over an energy barrier. In terms of the energy landscape it corresponds to crossing a saddle point [7]. In high temperature liquid the action of cutting or forming a bond was shown to be the elementary process of excitation [15, 19], and was named “anankeon” [19]. A typical Pachner move represents a bond exchange and involves two anankeons. They happen at unpredictable times, so that their dynamic is more efficiently described in terms of a Markov process. Hence the corresponding stress felt by each atom is constantly varying under the stress of circumstances, a concept that can be translated by the word “anagkeia” in Greek. Associated with this concept was the Greek goddess Ananke, expressing the fate or destiny, due to uncontrollable forces, constraints, and necessity. Hence the name “anankeon” associated with these stress-induced unpredictable atomic moves.

## **2.2. A Toy Model.**

What happens in the liquid state? Phonons still exist in liquids as in solids. However phonons with short wave lengths, comparable to the inter-atomic distance, are strongly damped in the liquid phase at high temperature. Whenever the typical time scale characterizing the anankeon dynamics is comparable to the phonon period, the phonon has no time to oscillate and it is overdamped. The present model investigates this damping more quantitatively. To proceed, the same intuition will be followed as in the original paper of Drude on electronic transport in metals [28]. In order to make the model computable, it will be assumed that it describes the mechanical fate of a given atom: (i) as long as the topology of atomic connectivity remain unchanged, this atom is located near the minimum of a local potential well, and it will oscillate, harmonically, with a frequency given by the local curvature of the well, (ii) then at random times (Poissonian distribution) the atom jumps, finding itself, after the jump in a new potential well, with a new local

curvature and a new initial location relative to the new equilibrium position and a new initial velocity (phase-space position). Hence, the curvature of potential well (expressed in terms of the frequency of oscillation) will be considered as a random variable with a fixed average and a given covariance  $\delta$ , which will be shown to be the most important parameter. Similarly, the new relative initial phase-space position, after the jump, will also be chosen randomly according to a Maxwell-Boltzmann distribution. To make the model even more computable, it will be assumed that only one degree of freedom of oscillation is allowed (local Einstein model). It will be seen that, even though this model is so simplistic, it exhibits a transition between two time-scales as  $\delta$  decreases. The computation of correlation functions, like viscosity, shows that this change of scale may affect the viscosity in an essential way.

### **2.3. Anankeons in Glass: the STZ-Theory.**

The deformation behavior of metallic glass was successfully described by the shear transformation zone (STZ) theory, proposed by Argon [29] and extended by Langer [30 – 33]. The idea is that during plastic deformation, the local groups of atoms form droplets, STZ, in which the solid really behaves like a liquid for a short time. Using the density of STZ as a variable, Langer et al. proposed a system of effective equation at the macroscopic scale that are modeling the behavior of the material under stress with a good accuracy. At the atomic scale numerical simulation show that these STZ's are the result of a cascade or avalanche of many atomic swaps, namely of anankeons, [34], starting at a random site, called the germ. Anankeon involves only two atoms which define the bond to be cut or formed, whereas STZ involves many (30 – 300) atoms [35, 36]. The initial anankeon action induces other anankeons in its neighborhood, because of the disruption created by the propagation of the stress induced by such swaps. The cascade looks like a local catastrophic event, occurring during a very short time, leading to the building of the local liquid-like droplets. The time scale representing the time necessary to create an STZ is however long in comparison with the typical time scale of the anankeon. Thus the cascade is not a collective phenomenon, but simply a succession of separate anankeon events induced by the stress field created by the preceding deformation events. A model for such a cascade of event was proposed in [34, 37].

### **3. Liquids at High Temperature as a Perfect Anankeon Gas**

In our approach the structure of glass or liquid is described by the Delone graph which specifies the topology of atomic connectivity. The Delone graph, however, does not have an energy scale, whereas in order to calculate thermodynamic properties we need the knowledge of the energy scale. A convenient way to introduce the energy scale to the Delone graph is to use the concept of the atomic-level stresses [38]. The atomic-level stress tensor for an atom  $i$ ,  $\bar{\sigma}_i$ , is defined by

$$\sigma_i^{\alpha\beta} = \frac{1}{V_i} \sum_j f_{ij}^\alpha r_{ij}^\beta, \quad (1)$$

where  $\alpha$  and  $\beta$  refer to Cartesian indices,  $V_i$  is the local atomic volume of atom  $i$ , and  $f_{ij}^\alpha$  and  $r_{ij}^\beta$  are the  $\alpha$  and  $\beta$  components of force and distance between atoms  $i$  and  $j$  [39, 40]. Its trace gives the atomic-level pressure

$$p_i = \frac{1}{3} (\sigma_i^{xx} + \sigma_i^{yy} + \sigma_i^{zz}), \quad (2)$$

whereas five other combinations give the shear, or deviatory, stresses,  $\tau_{ni}$ ,  $n = 1 \dots 5$ . The origin of the atomic-level stress is the atomic-level misfit between the size of the atom and the size and shape of the atomic site [38]. For instance if the atom is larger than the site it is placed it is under compressive pressure. Thus they are directly connected to the topology of the neighboring atoms which defines the size and shape of the atomic site. For instance the pressure is linearly related to the number of nearest neighbors, the coordination number [41].

The stress tensor has six components for each atom, however, because of the identity  $f_{ij} = -f_{ji}$ , the total number of free components is  $3N$ , equal to the positional degree of freedom. For this reason the equi-partition theorem holds for the stress in liquid [42, 43];

$$\frac{\langle p^2 \rangle}{2B} = \frac{\langle \tau_n^2 \rangle}{2G} = \frac{kT}{4}, \quad (3)$$

where  $B$  and  $G$  are the bulk and shear moduli. The distribution of local stress is Gaussian [44]. In the liquid state the atomic-level stresses fluctuate with time because the neighbors are dynamic. In high-temperature liquid phonons are overdamped, and the mechanism of structural change is ananeon excitation. Therefore a high-temperature liquid can be modeled as a free gas of ananeons. The degree of freedom associated with each ananeon will be given in terms of an atomic stress tensor. Their Gaussian distribution observed in the numerical results can be

interpreted in terms of a Gibbs state describing the thermal equilibrium in a statistical mechanical approach. If the atomic stress are uncorrelated, it becomes possible to compute the partition function  $Z(T;N)$  of a volume of liquid containing  $N$  atoms. Note, however, an anankeon excitation affects the stress tensors at two atoms involved in each atomic bond. Thus the part of the partition function regarding the potential energy is  $Z(T;N) = Z_1(T)^{N/2}$ , where

$$Z_1(T) = \int e^{-\beta \left( p^2/2B + \sum_n \tau_n^2/2G \right)} d\sigma, \quad \beta = \frac{1}{k_B T} . \quad (4)$$

The domain of integration is the space of all real symmetric  $d \times d$  matrices, representing a possible stress tensor. This Gaussian integral is easy to compute giving  $Z_1(T) = \mathbb{Z} T^{d(d+1)/4}$ , where  $\mathbb{Z}$  is a constant depending on  $B$  and  $G$ , but independent of the temperature. The Clausius entropy is given by  $S = k_B \ln(Z(N; T))$  leading to the following expression of the contribution of the potential energy to the heat capacity,  $C_{v,p} = c_d N k_B / 2$  where  $c_d = d(d+1)/4$ , which is 3 in 3D. Adding the contribution from the kinetic energy,  $C_{v,k} = c_d N k_B / 2$ , we obtain the total specific heat,  $C_v = c_d N k_B$ . Accordingly the system follows a Law of Dulong-Petit, just as the contribution of phonons in crystal. However, the physical origin is different in liquid, because the main degree of freedom associated with atoms are the atomic stress. Hence a liquid at high temperatures can be seen as a perfect gas of anankeons. This prediction gave a satisfactory answer to the experimental observation [45] of the saturation of the heat capacity at high temperature.

#### 4. Phonon-Anankeon Interaction

What happens at lower temperature, below the crossover temperature? The following model will show that as the temperature decreases, the vibration modes are constraining the shape of local clusters, so as to change the viscosity in a non-trivial way.

##### 4.1. Time Scales

Because the dynamics plays such an important role in explaining the difference between solids and liquids, the various relevant time scales ought to be discussed. The most elementary is  $\tau_{LC}$ , where  $LC$  stands for local configuration, representing the time required between two consecutive Pachner moves [14]. It corresponds to the anankeon relaxation time. The next time scale is called Maxwell relaxation time  $\tau_M = \eta/G_\infty$  [46] where  $\eta$  is the viscosity and  $G_\infty$  is the high frequency shear modulus. The Maxwell relaxation time represents the time scale below which the

system behaves like a solid and beyond which it can be considered as a liquid. Through classical as well as ab initio molecular dynamics simulation on various metallic liquids it was found that  $\tau_M = \tau_{LC}$  at high temperatures [17]. They obey the Arrhenius law,

$$\tau_M = \tau_{LC} = \tau_\infty e^{W/k_B T}. \quad (5)$$

However, below the crossover temperature,  $T_A (= T^*)$  the equality  $\tau_M = \tau_{LC}$  breaks down, and  $\tau_M$  becomes super-Arrhenius, whereas  $\tau_{LC}$  remains Arrhenius [47]. Near the glass transition point, there is a significant discrepancy between  $\tau_M$  and  $\tau_{LC}$ . This is the discrepancy that the present model is going to describe. It seems natural, then, to choose  $\tau_{LC}$  as the basic time scale for modeling.

#### 4.2. The toy model for anankeon-phonon interaction

There are two modes of dynamics for the atomic-level stresses. At high temperatures it is dominated by phonons. To describe phonons we adopt the Einstein model, and assume  $\omega_{E,i}$  is the local Einstein frequency of the atom  $i$ . Below  $T_A$  local configurational dynamics takes over [48]. For simplicity we also use the same Einstein model, but the values of  $\{\omega_{E,i}\}$  decrease rapidly with decreasing temperature. Around an atom anankeon excitation occurs randomly with the average interval of  $\tau_{LC}$ . Thus the distribution of the time interval between anankeon excitation should have an exponential distribution. Then the probability that anankeon is excited within the time  $\tau$  is,

$$P(\tau) = \frac{1}{\tau_{LC}} \int_0^\tau e^{-t/\tau_{LC}} dt. \quad (6)$$

Anankeon excitation involving the bond between atoms  $i$  and  $j$  changes the atomic-level stress tensor of the atom  $i$  and  $j$ ,  $\bar{\bar{\sigma}}_i$  and  $\bar{\bar{\sigma}}_j$ , and  $\omega_{E,i}$  and  $\omega_{E,j}$  by  $\Delta\omega_{i,n}$  and  $\Delta\omega_{j,n}$ . Here  $n$  denotes the sequence of anankeon excitation ( $-\infty < n < \infty$ ). It is reasonable to assume that  $\Delta\omega_{i,n}$  is also a random variable. Its average and variance are given by

$$\omega = \frac{1}{N} \sum_i \omega_{E,i}, \quad \Delta\omega = \left( \frac{1}{N} \sum_i (\Delta\omega_{i,n})^2 \right)^{1/2}. \quad (7)$$

#### 4.3. Viscosity

The viscosity is given by the fluctuation-dissipation theorem as [46]



$$\eta = \frac{V}{k_B T} \int C_\sigma(t) dt, \quad (8)$$

where  $V$  is the volume of the liquid,  $T$  temperature, and  $C_\sigma$  is a shear stress correlation function,

$$C_\sigma(t) = \langle \sigma^{xy}(0) \sigma^{xy}(t) \rangle. \quad (9)$$

In terms of the atomic-level stresses, eq. (1) [39],

$$\sigma^{xy}(t) = \frac{1}{V} \sum_i V_i \sigma_i^{xy}(t). \quad (10)$$

Therefore,

$$C_\sigma(t) = \frac{1}{V^2} \sum_{i,j} V_i V_j \langle \sigma_i^{xy}(0) \sigma_j^{xy}(t) \rangle. \quad (11)$$

Using the approximation in Ref. 48,

$$C_\sigma(t) = \frac{V}{V^2} \sum_i (V_i)^2 \langle \sigma_i^{xy}(0) \sigma_i^{xy}(t) \rangle, \quad (12)$$

where  $\nu \approx 2$ . In the liquid state the thermal average is equal for all atoms. Thus

$$C_\sigma(t) = \nu \langle \sigma_i^{xy}(0) \sigma_i^{xy}(t) \rangle. \quad (13)$$

We will show that  $C_\sigma(t) \sim \exp(-t/\tau_M)$ . For this purpose we compute the Laplace transform,

$$\tilde{L}C_\sigma(\zeta) = \int_0^\infty e^{-t\zeta} C_\sigma(t) dt. \quad (14)$$

Detailed derivation is given in Ref. 49 and summarized in Appendix 3. The result is

$$\tilde{L}C_\sigma(\zeta) = \frac{\tau a_2(\zeta)}{1 - a_2(\zeta) e^{-(\hat{p}_r^2 + 4/r^2)}}, \quad (15)$$

where

$$a_2(\zeta) = \left\langle \frac{1}{1 + \tau(\zeta + i2\omega_{j-1})} \right\rangle \approx \frac{1}{1 + \tau\zeta} + \mathcal{O}\left(\frac{1}{(1 + \tau\zeta)^2}\right) \quad (16)$$

To calculate  $a_2(\zeta)$  explicitly we need to know the distribution of  $\{\omega_j\}$ . Here for simplicity we assume that  $\{\omega_j\}$  are distributed evenly within the range of  $\omega \pm \sqrt{3}\delta$ . Then,

$$a_2(\zeta) = \frac{1}{i4\sqrt{3}z} \ln \left\{ \frac{1 + \tau(\zeta + 2i\omega) + i2\sqrt{3}z}{1 + \tau(\zeta + 2i\omega) - i2\sqrt{3}z} \right\}, \quad (17)$$

and  $z = \delta\tau$ . The value of  $z$  varies with temperature. At high temperatures the system samples wide space of potential energy landscape (PEL), so that the range of  $\{\omega_j\}$ ,  $\Delta\omega$ , is large, resulting in the value of  $z$  of the order of unity. As the system is cooled it gets settled in certain local basins in PEL, and the dynamics becomes more cooperative, dominated by configurational fluctuations because phonons are averaged out over the time  $\tau$ . Thus the values of  $\{\omega_j\}$  and  $\delta$  decrease rapidly with decreasing temperature. Thus cooling the system results in reducing the value of  $z$ . Now using the polar coordinates in the complex plane,

$$\rho e^{i\theta} = 1 + \tau \operatorname{Re}(\zeta) + i2\sqrt{3}z, \quad (18)$$

$$a_2(\zeta) = \frac{\theta}{2\sqrt{3}z}, \quad \tan \theta = \frac{2\sqrt{3}z}{1 + \tau \operatorname{Re}(\zeta)}. \quad (19)$$

Thus the solution critically depends on the value of  $z$ . If  $2\sqrt{3}z \geq \pi/2$ ,

$$\tau_M = \tau_{LC}, \quad (20)$$

whereas if  $2\sqrt{3}z < \pi/2$ ,

$$\frac{\tau_{LC}}{\tau_M} = 1 - \frac{2\sqrt{3}z}{\tan(2\sqrt{3}z)}. \quad (21)$$

The value of  $z$  varies with temperature, and

$$z = z_c = \frac{\pi}{4\sqrt{3}}, \quad (22)$$

defines the viscosity crossover temperature  $T_A = T^*$ . Above  $T_A$  eq. (20) holds, whereas below  $T_A$  eq. (21) applies.

## 5. Interpreting the Results

### 5.1. Crossover condition

Above  $T_A$  phonons are overdamped [17], so that at the critical value of  $z$ ,  $\omega\tau = 1$ . Then from eq. (22) the crossover condition is given by

$$\left. \frac{\Delta\omega}{\omega} \right|_c = \frac{\pi}{4\sqrt{3}} \approx 0.45. \quad (23)$$

The phonon frequency  $\omega$  depends on volume through the Grüneisen formula,

$$\frac{d \ln \omega}{d \ln V} = \gamma. \quad (24)$$

The Grüneisen constant is about 2 for many materials. Now for metallic systems with the random close packed (DRP) structure the coordination number  $N_C$  close to 12 ( $\sim 4\pi$  [50]), the volume strain,  $\varepsilon_v = \Delta \ln V$ , for changing the coordination number  $N_C$  by  $\frac{1}{2}$  is [38, 51]

$$\varepsilon_v^{crit} = 0.11, \quad (25)$$

thus activation of anankeon which changes  $N_C$  by unity will result in the volume strain of  $2\varepsilon_v^{crit} = 0.22$ . Therefore the change in  $\omega$  due to anankeon excitation is

$$\frac{\Delta\omega}{\omega} = \Delta \ln \omega = 2\gamma\varepsilon_v^{crit} = 0.44, \quad (26)$$

for  $\gamma = 2$ , quite close to the value in eq. (23). This agreement illustrates the reasonableness of the result expressed in eq. (21).

## 5.2 Glass transition

At low temperatures below the crossover temperature atomic dynamics become more correlated and cooperative. Therefore the anankeons become correlated, and the assumption of random sequence which led to eq. (21) breaks down. For instance when two atoms are surrounded by a glassy solid, breaking of a bond creates strong back stress field around the atoms which tries to restore the bond. In other word unlike the liquid above the crossover the system now has a memory and behaves like an anelastic solid. Consequently the effective value of  $z$  becomes smaller. It is difficult to estimate how  $z$  varies with temperature, but it should go to zero at the glass transition because the system is no longer dynamic. Therefore the overall change in  $\omega$  due to localized anankeon is of the order of  $1/N_C$ . For small values of  $z$ ,

$$\frac{\tau_M}{\tau_{LC}} = 1 / \left( 1 - \frac{2\sqrt{3}z}{\tan(2\sqrt{3}z)} \right) = \frac{1}{4z^2} + \dots \quad (27)$$

Thus  $\tau_M$  diverges at  $T_g$  ( $z = 0$ ), as expected. Strictly speaking, therefore,  $T_g$  is the ideal kinetic glass transition **Kauzmann** temperature where  $\tau_M$  diverges [52] rather than the kinetic-conventional glass transition temperature where  $\tau_M$  becomes comparable to the experimental time-scale. Also this result is based upon the lowest order term in eq. (16). In deeply supercooled liquid we will need to take higher order terms which make the results more complicated.

### 5.3 Fragility

Angell classified liquids into fragile and strong liquids, by plotting viscosity in the logarithmic scale against  $T_g/T$ , the so-called Angell plot [1]. In a very strong liquid, such as silica, the Arrhenius temperature dependence persists well above the glass transition up to very high temperatures. In our model this means  $z > z_c$  up to high temperatures. This is consistent with our model [51] in which the critical strain increases with decreasing  $N_C$ . Whereas there is no simple way to estimate the value of  $z$ , because the square of the phonon frequency is proportional to the local elastic constant  $C$  which scales with  $N_C$ , we may argue that,

$$z = \frac{\Delta\omega}{\omega} \approx \sqrt{\frac{\Delta C}{C}} \approx \sqrt{\frac{1}{N_C}}. \quad (28)$$

For  $N_C = 4$  we obtain  $z = 0.5$ , higher than the critical value  $z_c$ . Because silicate has an open structure cutting one bond does not affect other bonds even below  $T_A$ ; there is no back-stress effect. Thus the value of  $z$  should remain high through the supercooled state down to low temperatures, resulting in the Arrhenius behavior of viscosity with no crossover to the super-Arrhenius behavior.

### 5.4 Comparison with simulation

It is difficult to estimate how  $z$  depends on temperature. At the moment theories are not available to make such estimates, whereas it will require extensive simulation effort to do so. On the other hand, it is possible to gain some insight through the comparison of eq. (21) with the results of simulation in Ref. 17. We found that scaling of  $z$  by

$$1 - \frac{z}{z_c} = \left( \frac{1-t}{1-t_g} \right)^\gamma, \quad (29)$$

where  $t = T/T^*$ ,  $t_g = T_g/T^*$ ,  $T^* = 1.3 T_A$ ,  $\gamma = 4$ , of eq. (22) fits well to the simulation data as shown in Fig. 1. Because the physical meaning of this scaling is unclear, this agreement merely suggests that our model captures some features of the crossover phenomenon in spite of its simplicity. Here  $T^* > T_A$ , but this merely reflects the ambiguity of defining  $T_A$  from the viscosity data through the deviation from the Arrhenius behavior.

## 6. Conclusion

The origin of glass transition has long been debated, without satisfactory resolution. Whereas many research works focus on the glass transition itself, it is equally important to examine the crossover behavior of viscosity in a liquid at high temperatures. Below the crossover temperature,  $T_A$ , cooperative atomic dynamics leads to super-Arrhenius temperature dependence of viscosity, culminating inevitably to the glass transition. In our view this crossover occurs because of the competition between phonons and local configurational fluctuations represented by the action of cutting or forming atomic connectivity, called anankeons. In this article we propose a simplistic model of atomic dynamics in liquid, based on the concept of dynamic fluctuations in local atomic connectivity (anankeons), to elucidate the viscosity crossover phenomenon in the liquid phase. With this model it is possible to explain the crossover from a simple liquid to cooperative liquid and the divergence of viscosity near the glass transition temperature. The model is a mechanical analog of the Drude model for the electric transport in metal.

### **Acknowledgment**

JB was supported by NSF grant #DMS-1160962. TE was supported by the U.S. Department of Energy, Office of Science, Basic Energy Sciences, Materials Science and Engineering Division.

### **References**

1. C. A. Angell, Formation of Glasses from Liquids and Biopolymers, *Science*, **267**, No. 5206, 1924 (1995).
2. P. W. Anderson, Through the Glass Lightly, *Science*, **267**, No. 5204, 1615 (1995).
3. J. S. Langer, The mysterious glass transition, *Phys. Today* **60**, 2, 8 (2007).
4. D. R. Nelson, Order, frustration, and defects in liquids and glasses, *Phys. Rev. B* **28**, 5515 (1983).
5. T. R. Kirkpatrick and P. G. Wolynes, Connections between some kinetic and equilibrium theories of the glass transition. *Phys. Rev. A* **35**, 3072 (1987).
6. D. Kivelson, G. Tarjus, X. Zhao and S. A. Kivelson, Fitting of viscosity: Distinguishing the temperature dependences predicted by various models. *Phys. Rev. E* **53**, 751 (1996).
7. P. G. Debenedetti and F. H. Stillinger, *Nature* **410**, 259 (2001).

8. G. Tarjus, S. A. Kivelson, Z. Nussinov and P. Viot, The frustration-based approach of supercooled liquids and the glass transition: a review of critical assessment. *J. Phys. Cond. Mat.* **17**, R1143 (2005).
9. W. Götze, *Complex dynamics of glass-forming liquids* (Oxford University Press, Oxford, 2009).
10. M. E. Blodgett, T. Egami, Z. Nussinov and K. F. Kelton, Proposal for Universality in the Viscosity of Metallic Liquids, *Scientific Reports*, **5**, 13837 (2015).
11. P. J. Steinhardt, D. R. Nelson and M. Ronchetti, Icosahedral bond orientational order in supercooled liquids, *Phys. Rev. Lett.* **47**, 1297 (1981).
12. A. I. Goldman and K. F. Kelton, Quasicrystals and crystalline approximants, *Rev. Mod. Phys.* **65**, 213 (1993).
13. H. Tanaka, T. Kawasaki, H. Shintani and K. Watanabe, Critical-like behavior of glass-forming liquids, *Nature Mater.* **9**, 324 (2010).
14. Y. S. Elmatad, D. Chandler and J. P. Garrahan, Corresponding states of structural glass formers. *J. Phys. Chem. B* **113**, 5563 (2009).
15. K. S. Schweitzer and E. J. Saltzman, Entropic barriers, activated hopping, and the glass transition in colloidal suspensions. *J. Chem. Phys.* **119**, 1181 (2003).
16. M. Maiti and M. Schmiedeberg, Ergodicity breaking transition in a glassy soft sphere system at small but non-zero temperatures. *Sci. Rep.* **8**:1837 (2018).
17. T. Iwashita, D. M. Nicholson, and T. Egami, Elementary excitations and crossover phenomenon in liquids. *Phys. Rev. Lett.* **110**, 205504 (2013).
18. J. D. Bernal, A geometrical approach to the structure of liquids, *Nature*, **183**, 141 (1959).
19. T. Egami, Elementary excitation and energy landscape in simple liquids. *Mod. Phys. Lett. B*, **28**, 1430006 (2014).
20. P. D. Schall, A. Weitz and F. Spaepen, Structural rearrangements that govern flow in colloidal glasses, *Science* **318**, 1895 (2007).
21. W. Dmowski, S. O. Diallo, K. Lokshin, G. Ehlers, G. Ferré, J. Boronat and T. Egami, Observation of dynamic atom-atom correlation in liquid helium in real space, *Nature Commun.*, **8**, 15294 (2017).
22. B. E. Warren, *X-ray diffraction* (Addison-Wesley, Reading, 1969).

23. J. D. Bernal, The Bakerian Lecture, 1962: The structure of liquids, *Proc. Roy. Soc. London*, **280**, 299 (1964).
24. F. Aurenhammer and R. Klein, "Voronoi diagrams", in Handbook of computational geometry, 201290, North-Holland, Amsterdam, (2000).
25. F. Aurenhammer, R. Klein and D. T. Lee, Voronoi diagrams and Delaunay triangulations. (World Scientific Publishing Co. Pte. Ltd., Hackensack, N J, 2013).
26. J. Bellissard, Delone Sets and Material Science: a Program, in Mathematics of Aperiodic Order, J. Kellendonk, D. Lenz, J. Savinien, Eds. *Progress in Mathematics*, Series, 309, Birkhäuser, (2015).
27. U. Pachner, P. L. homeomorphic manifolds are equivalent by elementary shellings, *European J. Combin.*, **12**, (1991), 129-145.
28. P. Drude, Zur Elektronentheorie der Metalle, *Ann. Phys.*, **1**, 566 (1900) ; *Ann. Phys.*, **3**, 369 (1900).
29. A. S. Argon, Plastic deformation in metallic glasses, *Acta Metall.* **27**, 47 (1979).
30. M. L. Falk, and J. S. Langer, Dynamics of viscoplastic deformation in amorphous solids, *Phys. Rev. E* **57**, 7192 (1998).
31. J. S. Langer and L. Pechenik, Dynamics of shear-transformation zones in amorphous plasticity: Energetic constraints in a minimal theory", *Phys. Rev. E*, **68**, 061507 (2003).
32. J. S. Langer, Dynamics of shear-transformation zones in amorphous plasticity: Formulation in terms of an effective disorder temperature, *Phys. Rev. E*, **70**, 041502 (2004).
33. J. S. Langer, Shear-transformation-zone theory of deformation in metallic glasses, *Scripta Mater.* **54**, 375 (2006).
34. Y. Fan, T. Iwashita and T. Egami, Crossover from localized to cascade relaxations in metallic glasses, *Phys. Rev. Lett.*, **115**, 045501 (2015).
35. J. D. Ju, D. Jang, A. Nwankpa and M. Atzmon, An atomically quantized hierarchy of shear transformation zones in a metallic glass. *Journal of Applied Physics* **109**, 053522 (2011).
36. D. Pan, A. Inoue, T. Sakurai and M. W. Chen, Experimental characterization of shear transformation zones for plastic flow of bulk metallic glasses. *Proc. Nat. Acad. Sci.* **105**, 14769 (2008).
37. Y. Fan, T. Iwashita, and T. Egami, Energy landscape-driven nonequilibrium evolution of inherent structure in disordered material, *Nature Commun.*, **8**, 15417 (2017).

38. T. Egami, Atomic Level Stresses, *Progr. Mater. Sci.* **56**, 637 (2011).
39. T. Egami, K. Maeda and V. Vitek, Structural defects in amorphous solids. A computer simulation study, *Phil. Mag. A*, **41**, 883 (1980).
40. M. Born and K. Huang, *Dynamical Theory of Crystal Lattices* (Clarendon Press, Oxford, 1954).
41. T. Egami and D. Srolovitz, Local structural fluctuations in amorphous and liquid metals: a simple theory of the glass transition, *J. Phys. F: Met. Phys.*, **12**, 2141 (1982).
42. S.-P. Chen, T. Egami and V. Vitek, Local fluctuations and ordering in liquid and amorphous metals, *Phys. Rev. B* **37**, 2440 (1988).
43. V. A. Levashov, R. S. Aga, J. R. Morris and T. Egami, Equipartition theorem and the dynamics of liquids, *Phys. Rev. B*, **78**, 064205 (2008).
44. D. Srolovitz, K. Maeda, V. Vitek and T. Egami, Structural defects in amorphous Solids; Statistical analysis of a computer model, *Philos. Mag. A* **44**, 847 (1981).
45. H. S. Chen, D. Turnbull, Evidence of a glass-liquid transition in a gold, germanium silicon alloy, *J. Chem. Phys.*, **48**, 2560 (1968).
46. J.-P. Hansen and I. R. McDonald, *Theory of simple liquids*, 3<sup>rd</sup> ed. (Academic Press, Amsterdam, 2006).
47. T. Iwashita and T. Egami, Local energy landscape in simple liquids”, *Phys. Rev. E*, **90**, 052307 (2014).
48. V. A. Levashov, J. R. Morris and T. Egami, The origin of viscosity as seen through atomic level stress correlation function, *J. Chem. Phys.* **138**, 044507 (2013).
49. Jean V. Bellissard, Anankeon theory and viscosity of liquids: A toy model, arXiv: 1708.06624v1, (Aug. 19, 2017).
50. T. Egami and S. Aur, Local atomic structure of amorphous and crystalline alloys: Computer simulation, *J. Non-Cryst. Solids* **89**, 60 (1987).
51. T. Egami, Universal criterion for metallic glass formation, *Mater. Sci. Eng. A* **226-228**, 261 (1997).
- ~~52. W. Kauzmann, The nature of the glassy state and the behavior of liquids at low temperatures, *Chem. Rev.* **43**, 219 (1948).~~
- 53.52. Y. Fan, T. Iwashita and T. Egami, How thermally induced deformation starts in metallic glass, *Nature Commun.*, **5**, 5083 (2014).





**Figure caption:**

Figure 1. Plot of  $\tau_M/\tau_{LC}$  against  $T/T_A$ , circles by simulations for various models from Ref. 17, the line by eq. (21) with the temperature scaling of eq. (29).

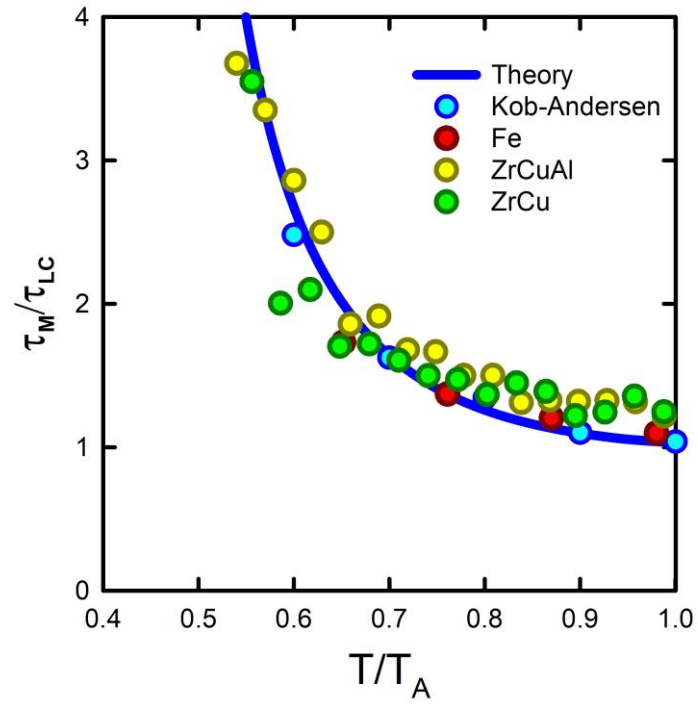


Fig. 1

## Appendix I. The Delone Hypothesis and the Ergodic Paradox.

An instantaneous snapshot of the atomic arrangement can be described as a set of points  $L$ , representing the position of atomic nuclei. With a very good approximation  $L$  is efficiently described as a Delone set. Namely it is characterized by two length scales  $0 < r_R < 1$  defined as follows: (i) any open Euclidean ball of radius  $r$  contains at most one point of  $L$ , (ii) any closed Euclidean ball of radius  $R$  contains at least one point of  $L$ . The first condition is equivalent to having a minimum distance  $2r$  between any pair of distinct atoms. The second condition is equivalent to forbidding holes a diameter larger than  $2R$ . However, the principles of Equilibrium Statistical Mechanics and the ergodicity with respect to translations contradict such a hypothesis. This is the content of the so-called Ergodicity Paradox [26]. This is because in the infinite volume limit, the ergodic theorem implies that with probability one, given any  $\varepsilon > 0$ , somewhere in the atomic configuration two atoms are at a distance shorter than  $\varepsilon$ . Similarly, with probability one, given any  $\varepsilon > 0$ , somewhere in the atomic configuration there is a hole of size larger than  $1/\varepsilon$ . However, such local arrangement are rare, so that dynamically their lifetime is so short that they are unobservable. Hence restricting the atomic configurations to make up a Delone set is a reasonable assumption called the Delone Hypothesis

## Appendix 2. Voronoi Tiling, Delone Graphs and Local Topology.

Given a Delone set  $L$  and a point  $x \in L$ , the Voronoi cell  $V(x)$  is defined as the set of points in space closer to  $x$  than to any other point in  $L$ .  $V(x)$  can be shown to be the interior of a convex polyhedron containing the open ball centered at  $x$  of radius  $r$  and contained in the ball centered at  $x$  of radius  $R$  [24, 25]. The closure  $T(x)$  of the Voronoi cell is called a Voronoi tile. Two such tiles can only intersect along a common face. In particular two Voronoi cells centered at two distinct points of  $L$  do not intersect. The entire space is covered by such tiles, so that the family of Voronoi tiles constitute a tiling, the Voronoi tiling. The vertices of the Voronoi tiles will be called Voronoi points. Their set  $L^*$  is usually called the dual lattice. For a generic atomic configuration, a Voronoi point has not more than  $d + 1$  atomic neighbors in space-dimension  $d$  (3 in the plane and 4 in the space). In particular, the Voronoi points are the center of a ball with  $d + 1$  atoms on its boundary, a property called by Delone (who signed Delaunay) the “empty sphere property” [11]. It means that it is at the intersection of  $d + 1$  Voronoi tiles. The  $d + 1$  atoms located at the center of those

tiles are the vertices of a simplex (triangle for  $d = 2$ , tetrahedron for  $d = 3$ ) that generates the so-called Delaunay triangulation.

Two points  $x, y \in \mathbf{L}$  will be called nearest neighbors whenever their respective Voronoi tiles are intersecting along a facet, namely a face of codimension 1. The pair  $\{x, y\}$  will be called an edge. In practice, though, using physical criteria instead of a geometrical one, an edge might be replaced by the concept of bond, to account for the fact that the atoms associates with  $x$  and  $y$  are strongly bound [18, 23]. The term “strongly” is defined through a convention about the binding energy, so as to neglect bonds between atoms weakly bound to each other. Whatever the definition of an edge, geometrical or physical (bonds), this gives the Delone graph  $G = (\mathbf{L}, \mathbf{E})$ , where  $\mathbf{L}$  plays the role of the vertices and  $\mathbf{E}$  denotes the set of edges or of bonds. At this point the Delone graph needs not being oriented.

Along a graph, a path is an ordered finite set of edges, each sharing a vertex with its successor or with its predecessor. The number of such edges is the length of the path. The graph-distance between two vertices is the length of the shortest paths joining them. A graph-ball centered at  $x$  of radius  $n$  will be the set of all vertices at graph distance at most  $n$  from  $x$ . Such graph balls correspond to local clusters. Two graph balls are called isomorphic if there is a one-to-one surjective map between their set of vertices, which preserve the graph distance. As a result, if the atomic positions is slightly changed locally in space, the graph balls might still be isomorphic. Therefore graph ball, modulo isomorphism are encoding what physicists called the local topology of the atomic configuration. The transition between two graph balls can be described precisely through the concept of Pachner moves [24, 25, 27]. This concept was created by experts of computational geometry, to describe the deformation of manifolds via a computer. A Pachner moves can only occur if at least one Voronoi point becomes degenerate, namely it admits at least  $d + 2$  atomic neighbor at some point during the move. Such moves correspond to a local change in a graph ball, namely an edge disappear another may reappear. A Pachner move corresponds exactly to the concept of anankeon. It can be described through using the Delaunay triangulation as explained in Fig. A1. A recent simulation [5352] indeed show that the average number of atoms involved in the saddle point (a mid-point of Pachner move) is five for  $d = 3$ .

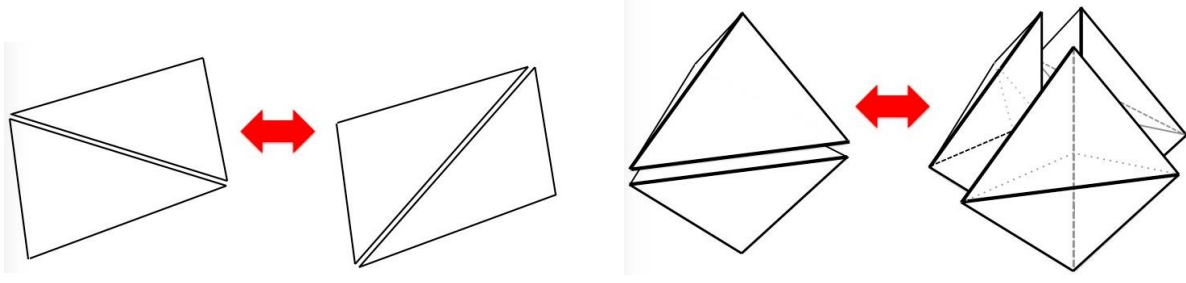


Figure A1. Left: a Pachner move in the plane. Right: a Pachner move in the 3-space. In 3D-space such a move involves at least five atoms moving quickly to deform the Delaunay triangulation, changing the nature of the Delone graph, namely the local topology. This number five has been seen in numerical simulations [5352].

### Appendix 3. Derivation of eq. (16) [see [49] for full details]

We assume that the atomic-level shear stress varies with time for two different ways, by phonon and by anankeon. The phonon dynamics is harmonic, and for simplicity we use one local phonon frequency for each atom,  $\omega_{Ei}$  (Einstein model). The anankeon excitation produces local change in the value of  $\omega_{Ei}$  by  $\Delta\omega_{Ei}$ . To describe the temporal evolution of the atomic-level shear stress,  $\sigma_i^{xy}(t)$ , we define  $\mathbf{X}(t) = (u, v)$ , where  $u = \sigma_i^{xy}(t)$  and  $v = du/dt$ . We also define  $f(\mathbf{X}) = u$ . The continuous evolution of  $\mathbf{X}(t)$  is given by

$$\mathbf{X}(t + dt) = e^{-\omega dt \mathbf{J}} \mathbf{X}(t), \quad -\mathbf{J} = v\partial_u - u\partial_v. \quad (\text{A1})$$

We now consider a series of anankeon operations at time  $\tau_j$ , ( $j = 0, 1, 2, \dots, n$ ). By definition  $\tau_{n+1} - \tau_n > \tau_{LC}$ . For each anankeon excitation  $\mathbf{X}$  makes a jump;

$$\mathbf{X}(\tau_j + 0) = \mathbf{X}(\tau_j - 0) + \boldsymbol{\xi}_j. \quad (\text{A2})$$

Therefore,

$$f(\mathbf{X} + \boldsymbol{\xi}) = e^{\boldsymbol{\xi} \cdot \nabla} f(\mathbf{X}), \quad \boldsymbol{\xi} \cdot \nabla = a\partial_u + b\partial_v, \quad (\text{A3})$$

where  $\boldsymbol{\xi} = (a, b)$ . Then,

$$f(\mathbf{X}(t)) = \prod_{j=1}^n \left( e^{-(\tau_j - \tau_{j-1})\omega_{j-1}J} e^{\xi_j \cdot \nabla} \right) e^{-(t - \tau_n)\omega_n J} f(\mathbf{X}(0)). \quad (\text{A4})$$

Now we break up the Laplace transform, eq. (15), into time segments of  $\tau_n$ ,

$$\tilde{L}C_\sigma(\zeta) = \nu \sum_{n=0}^{\infty} \left\langle f(\mathbf{X}(0)) \int_{\tau_n}^{\tau_{n+1}} e^{-t\zeta} f(\mathbf{X}(t)) dt \right\rangle. \quad (\text{A5})$$

From eq. (A4),

$$\tilde{L}C_\sigma(\zeta) = \nu \sum_{n=0}^{\infty} \left\langle f(\mathbf{X}(0)) \prod_{j=1}^n \left( e^{-(\tau_j - \tau_{j-1})\omega_{j-1}J} e^{\xi_j \cdot \nabla} \right) e^{-(t - \tau_n)\omega_n J} f(\mathbf{X}(0)) \right\rangle. \quad (\text{A6})$$

Because  $\{\tau_j\}$  obeys the Poisson statistics,

$$\left\langle e^{-(\tau_j - \tau_{j-1})A} \right\rangle = \int_0^{\infty} e^{-s/\tau - sA} \frac{ds}{\tau} = \frac{1}{1 + \tau A}. \quad (\text{A7})$$

where  $\tau = \langle \tau_j - \tau_{j-1} \rangle = \tau_{LC}$ . This is a crucial step in this theory. Then eq. (A6) becomes,

$$\tilde{L}C_\sigma(\zeta) = \nu \tau \sum_{n=0}^{\infty} \left\langle f(\mathbf{X}(0)) \prod_{j=1}^n \left( \frac{1}{1 + \tau(\zeta + \omega_{j-1}J)} e^{\xi_j \cdot \nabla} \right) \frac{1}{1 + \tau(\zeta + \omega_n J)} f(\mathbf{X}(0)) \right\rangle. \quad (\text{A8})$$

Because  $\xi_j$ 's and  $\omega_j$ 's are statistically independent, averages are,

$$\left\langle e^{\xi_j \cdot \nabla} \right\rangle = e^{k_B T \nabla^2 / 2m}. \quad (\text{A9})$$

Defining,

$$\mathbf{A}(\zeta) = \left\langle \frac{1}{1 + \tau(\zeta + \omega_{j-1}J)} \right\rangle, \quad (\text{A10})$$

we obtain,

$$\tilde{L}f(\zeta) = \nu \tau \sum_{n=0}^{\infty} \left\{ \mathbf{A}(\zeta) e^{k_B T \nabla^2 / 2m} \right\}^n \mathbf{A}(\zeta) f(\mathbf{X}(0)) = \frac{\nu \tau}{1 - \mathbf{A}(\zeta) e^{k_B T \nabla^2 / 2m}} \mathbf{A}(\zeta) f(\mathbf{X}(0)). \quad (\text{A11})$$

Now, using the polar coordinate

$$f_\ell(\mathbf{X}) = e^{i\ell\theta} f(|\mathbf{X}|), \quad (\text{A12})$$

and choosing  $\ell = \pm 2$  for the symmetry of shear, we find that the kernel of (A10),  $1/(1 + \tau(\zeta + \omega_{j-1}J))$ ,

has a pole at

$$\zeta_{\pm 2} = -\left( \frac{1}{\tau} \pm i2\omega_{j-1} \right). \quad (\text{A13})$$

Thus,

$$a_{\pm 2}(\zeta) = \left\langle \frac{1}{1 + \tau(\zeta \pm i2\omega_{j-1})} \right\rangle \approx \frac{1}{1 + \tau\zeta} + \mathcal{O}\left(\frac{1}{(1 + \tau\zeta)^2}\right), \quad (\text{A14})$$

To calculate  $a_2(\zeta)$  explicitly we need to know the distribution of  $\{\omega_j\}$ . Here for simplicity we assume that  $\{\omega_j\}$  are distributed evenly within the range of  $\omega \pm \sqrt{3}\delta$ . This assumption leads to eqs. (18) to (21).